

Supporting Information

Superior flexibility of wrinkled carbon shell under electrochemical cycling

*Qianqian Li^{a‡}, Peng Wang^{a‡}, Qiong, Feng^a, Minmin Mao^b, Jiabin Liu^c, Hongtao Wang^{a*1}, Scott X. Mao^{d*}, Xi-Xiang Zhang^{e*}*

^a Institute of Applied Mechanics, Zhejiang University, Hangzhou 310027, China.

^b Department of Materials Science and Engineering, State Key Laboratory of Silicon Materials, Zhejiang University, Hangzhou 310027, China.

^c College of Electrical Engineering, Zhejiang University, Hangzhou 310027, China

^d Department of Mechanical Engineering and Materials Science, University of Pittsburgh, Pittsburgh, Pennsylvania 15261, United States.

^e Advanced Nanofabrication, Imaging and Characterization Core Laboratory, King Abdullah University of Science and Technology, Thuwal 239955, Kingdom of Saudi Arabia

¹All correspondence should be addressed to htw@zju.edu.cn; sxm2@pitt.edu and xixiang.zhang@kaust.edu.sa

[‡] Both authors contributed equally to this work.

Supporting Figures

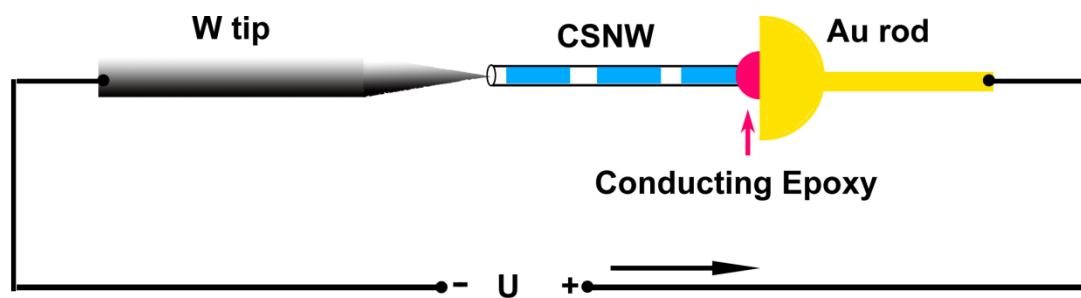


Fig. S1 Schematic illustration of the experimental setup for in situ WCS fabrication, mechanical tests and I - V measurements. For *in situ* electrochemical test, the tungsten tip was replaced by a cathode covered with a bulk of Li metals. The Li metal is unavoidably exposed to air during handling. It is expected the surface layer is oxidized into Li_2O , which serves as solid electrolyte for the half-cell LIB configuration.

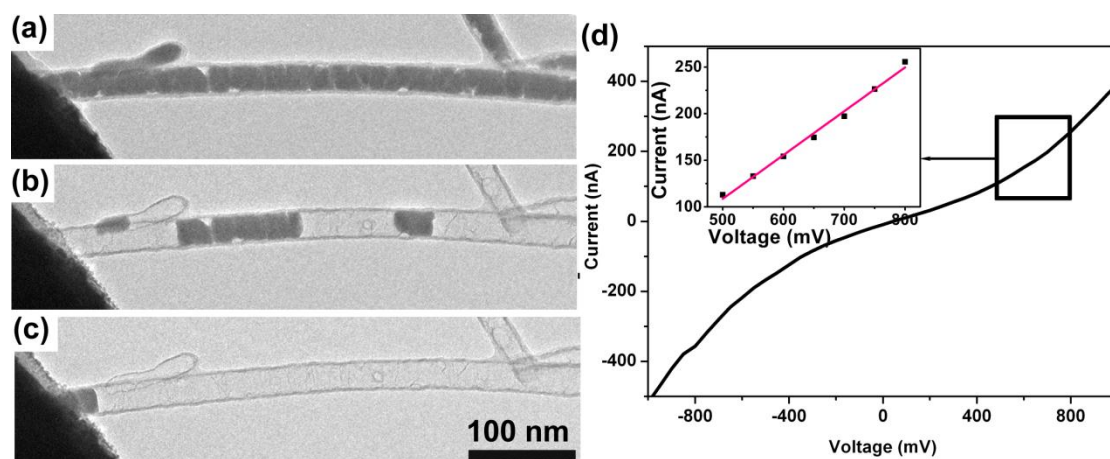


Fig. S2 *In situ* fabrication of a WCS. (a) The tungsten electrode was brought into contact a CSNW; (b – c) The Sn core was slowly removed by Joule heating. (d) $I - V$ curve of the as-fabricated WCS.

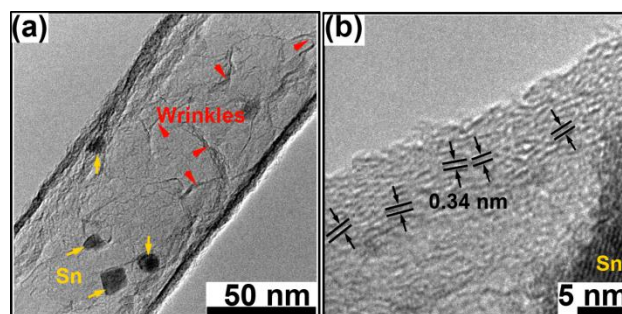


Fig. S3 Characterization for the wrinkle carbon shell. (a) The typical of the carbon shell with some unevaporated tin particles shown by the yellow arrows, and wrinkles shown by the red arrows. (b) HRTEM of carbon shell with spacing about 0.34 nm, indicating good crystallinity.

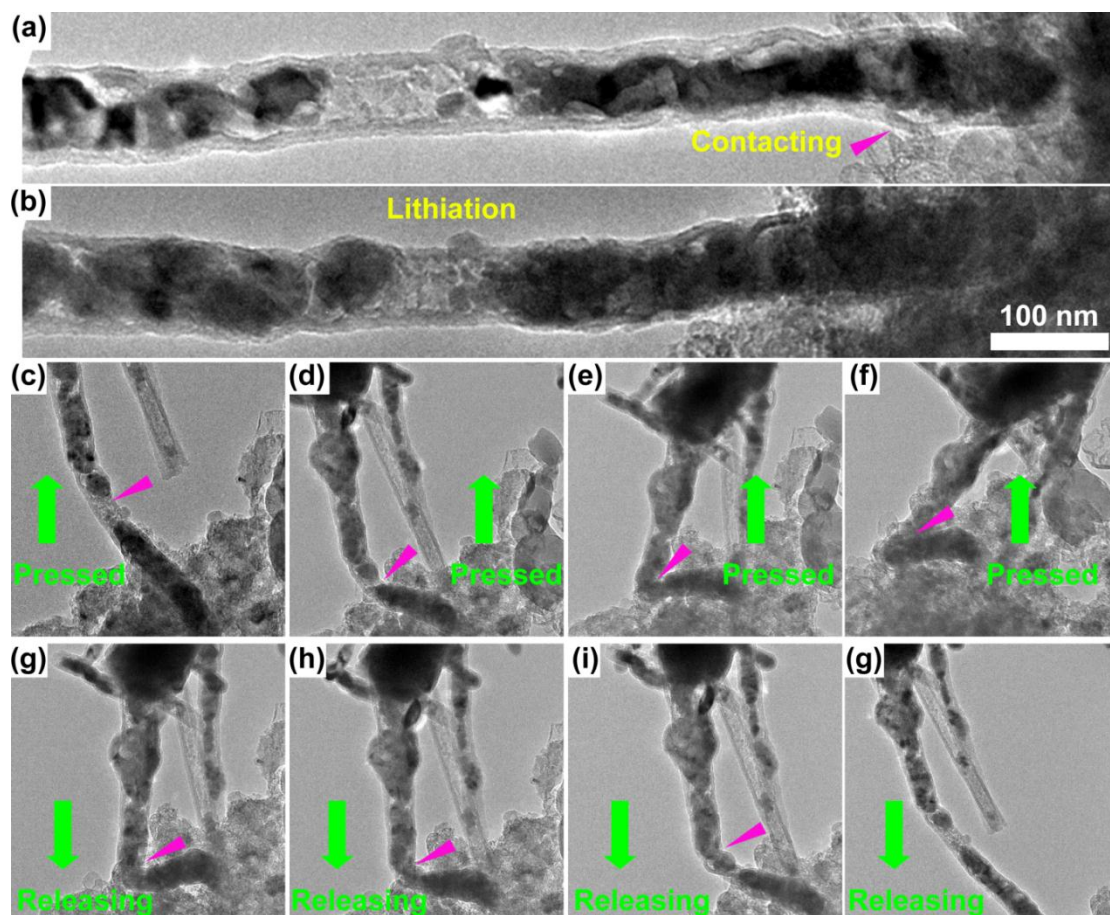


Fig. S4 Mechanical test on a lithiated CSNW. TEM images of a CSNW before (a) and after (b) lithiation. (c – j) The structural evolution of the lithiated CSNW under compression.

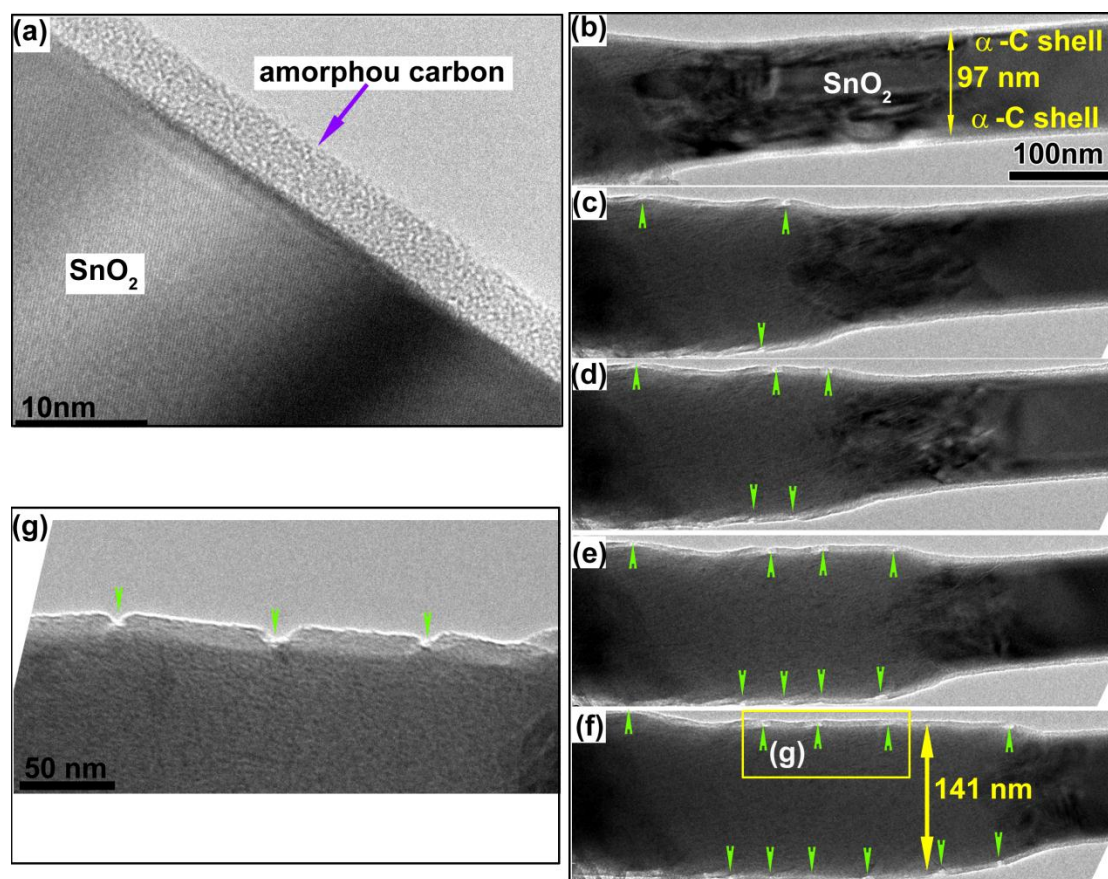


Fig. S5 (a) HRTEM image of an amorphous carbon coated SnO₂ nanowire. No graphitic lattice fringes were observed in the shell. (b-f) Morphology evolution of an amorphous carbon coated nanowire electrode during an electrochemical cycle. (g) After full lithiation, the radius expansion is about 156%, which leads to fracture (as indicated by the arrow heads) of the amorphous carbon shell due to its brittle nature.

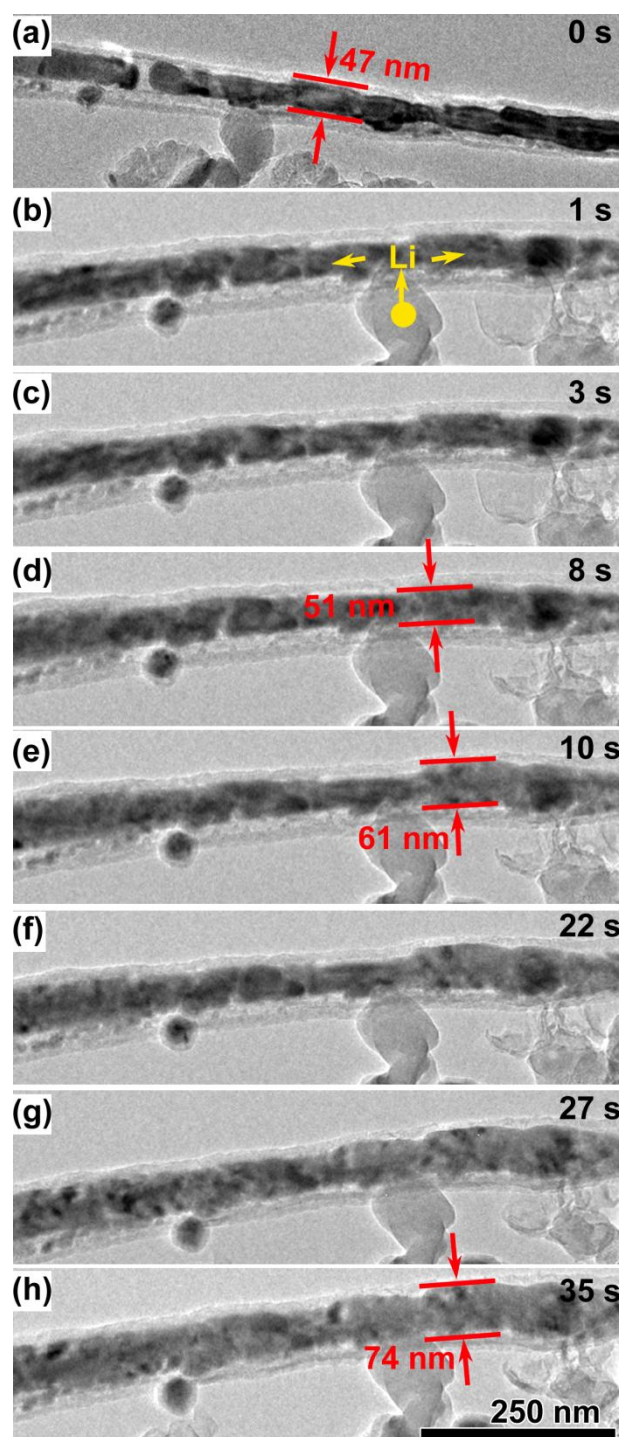


Fig. S6 Structural evolution of a CSNW during lithiation. (a) The Li/Li₂O cathode was brought into contact with the sidewall of a CSNW; (b) The contrast change in the Sn core indicated instantaneous start of lithiation; (c – h) The diameter of the Sn core increased from about 47 nm to 74 nm in a time span of 35 s.

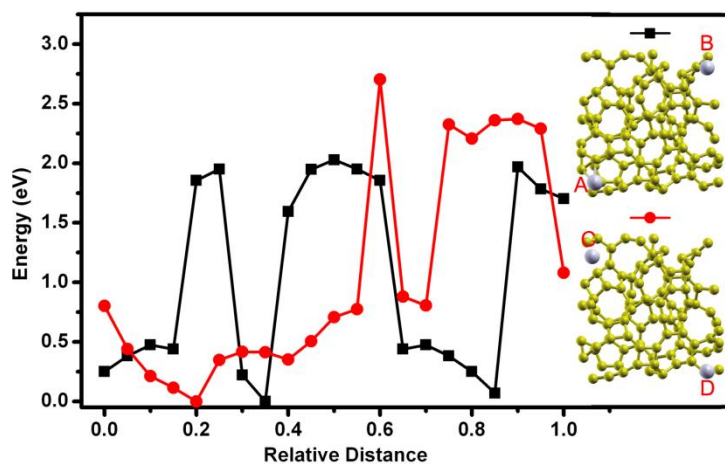


Fig. S7 Energy profile of lithium ions migrating on the surface of the amorphous carbon. The amorphous structure was constructed by melting a bulk of diamond and subsequently quickly being quenched to room temperature, using the molecular dynamics simulation. The energy profiles of surface diffusion are calculated by using the nudged elastic band (NEB) method in the frame of DFT. The migration paths are chosen to be from A to B and from C to D.